Atmos. Chem. Phys. Discuss., 10, 30347–30379, 2010
www.atmos-chem-phys-discuss.net/10/30347/2010/
doi:10.5194/acpd-10-30347-2010

Atmospheric Chemistry and Physics Discussions

Impact of model grid spacing on regional- and urban-scale air quality predictions of organic aerosol

C. A. Stroud[1], P. A. Makar[1], M. D. Moran[1], W. Gong[1], S. Gong[1], J. Zhang[1], K. Hayden[1], C. Mihele[1], J. R. Brook[1], J. G. Abbatt[2], and J. P. D. Slowik[2]

[1]Air Quality Research Division, Environment Canada, Toronto, Canada
[2]Department of Chemistry, University of Toronto, Toronto, Canada

Received: 22 October 2010 – Accepted: 12 November 2010 – Published: 13 December 2010

Correspondence to: C. A. Stroud (craig.stroud@ec.gc.ca)

Published by Copernicus Publications on behalf of the European Geosciences Union.

Abstract

Regional-scale chemical transport model predictions of urban organic aerosol to date tend to be biased low relative to observations, a limitation with important implications for applying such models to human exposure health studies. We used a nested version of Environment Canada's AURAMS model (42-to-15-to-2.5 km nested grid spacing) to predict organic aerosol concentrations for a temporal and spatial domain corresponding to the Border Air Quality and Meteorology Study (BAQS-Met), an air-quality field study that took place in the southern Great Lakes region in the summer of 2007. The use of three different horizontal grid spacings allowed the influence of this parameter to be examined. A domain-wide average for the 2.5 km domain and a matching 15 km subdomain yielded very similar organic aerosol averages (4.8 vs. 4.3 $\mu g\,m^{-3}$, respectively). On regional scales, secondary organic aerosol dominated the organic aerosol composition and was adequately resolved by the 15 km model simulation. However, the shape of the organic aerosol concentration histogram for the Windsor urban station improved for the 2.5 km simulation relative to those from the 42 and 15 km simulations. The model histograms for the Bear Creek and Harrow rural stations were also improved in the high concentration "tail" region. As well the highest-resolution model results captured the midday 4 July organic-aerosol plume at Bear Creek with very good temporal correlation. These results suggest that accurate simulation of urban and large industrial plumes in the Great Lakes region requires the use of a high-resolution model in order to represent urban primary organic aerosol emissions, urban VOC emissions, and the secondary organic aerosol production rates properly. The positive feedback between the secondary organic aerosol production rate and existing organic mass concentration is also represented more accurately with the highest-resolution model. Not being able to capture these finer-scale features may partly explain the consistent negative bias reported in the literature when urban-scale organic aerosol evaluations are made using coarser-scale chemical transport models.

ACPD

10, 30347–30379, 2010

1 Introduction

Atmospheric aerosols have important human health impacts and are estimated to cause more than a million premature deaths globally per year (Davidson et al., 2005). Organics comprise approximately half of atmospheric $PM_{2.5}$ (particulate matter with aerodynamic diameter less than 2.5 µm) and may be a major player in the aerosol health effects. Ambient data indicate that oxygenated organic aerosol (OOA) comprises a large faction of the organic aerosol (OA) (Zhang et al., 2007). However, our understanding of the origin, transformation, and fate of OOA is poorly known. As a result, our understanding of the atmospheric OA budget is highly uncertain (Goldstein and Galbally, 2007; Hallquist et al, 2009).

Air quality (AQ) modelling systems have been developed to provide numerical forecasts of pollutant concentrations given specified emissions of the pollutants or their precursors. Modelling studies to date, however, have generally under-predicted OA concentrations, especially in urban air masses (Griffin et al., 2005; Heald et al., 2005; Chen et al., 2006; McKeen et al., 2007; Ying et al., 2007; Yu et al., 2007; Carlton et al., 2008; Murphy and Pandis, 2009; Smyth et al., 2009). There have been a number of hypotheses proposed to explain these model under-predictions, namely (1) unaccounted-for intermediate volatile organic compounds (i.e., $10^4 < C^* < 10^6$ µg m^{-3}, where C^* is the effective saturation concentration of the IVOC) in the emissions inventories considered, (2) evaporation of semi-volatile organic compounds (SVOCs, $10^1 < C^* < 10^4$ µg m^{-3}) followed by gas-phase oxidation and condensation as secondary organic aerosol (SOA), (3) unaccounted-for biogenic VOC emissions, (4) aerosol-phase chemistry decreasing the volatility of products, (5) aqueous-phase aerosol and cloud chemistry increasing the solubility of products, and (6) "older" SOA yield data collected with slower response and higher detection limit instrumentation. Recent results from the SAPRC99-PMCAM$_x$-VBS modelling system (Tsimpidi et al., 2009) address some of these processes (points 1, 2, 6).

ACPD
10, 30347–30379, 2010

One more explanation that may affect modelled OA is model horizontal grid-cell spacing and its impact on resolving emissions of organic compounds, meteorology, and chemistry. First, it is well known that significant artificial diffusion occurs when emissions from compact sources such as point or line sources are injected into a larger model grid cell (e.g., Gillani and Pleim, 1996; Karamchandani et al., 2002). The magnitude of the artificial diffusion is directly proportional to the grid-cell size. Second, the representation of transport processes is also affected by grid spacing, since small-scale circulations may not be resolved well or at all for coarse grid spacing, a particular concern for regions of complex terrain such as the Great Lakes region of North America (e.g., Levy et al., 2010). Third, chemistry can also be affected by grid spacing, since chemical reactions in subgrid-scale plumes are unlikely to be accurately represented, given that chemical species within a single plume will be at least partially isolated from the ambient chemical environment of the grid cell and that two plumes of reacting species may overlap or may remain separated. This dependence has led to the development of a number of plume-in-grid approaches to represent chemistry in subgrid-scale plumes (e.g., Kumar and Russell, 1996; Karamchandani et al., 2006).

For example, Jang et al. (1995a, b) found that AQ models employing coarser grid spacing tended to underpredict ozone maxima because ozone precursors were diluted too much and to overpredict ozone minima because the representation of the NO titration process was too weak. Gillani and Pleim (1996) suggested that improved representations of urban plumes could only be achieved for horizontal grid spacing less than 20 km. Cohan et al. (2006) suggested that to predict regional ozone patterns, the grid spacing used should be on the order of 12 km or less to represent ozone production and loss processes accurately. Karamchandani et al. (2002, 2006) noted that the formation of inorganic PM species such as sulphate and nitrate in a large NO_x plume will be significantly slower than in the surrounding air due to oxidant limitations. Since OA has both primary and secondary sources, it is reasonable to expect that modelled OA concentrations may also display some dependence on model horizontal grid spacing.

ACPD
10, 30347–30379, 2010

The Border Air Quality and Meteorology Study (BAQS-Met) took place in summer 2007 in the southern Great Lakes region of North America. High temporal resolution OA data were collected in southwestern Ontario at two ground sites and on board the instrumented Convair aircraft and CRUISER (Canadian Regional and Urban Investigation System for Environmental Research) mobile truck. Important local emissions of primary OA and OA precursors include mobile, area, and point sources in the Greater Detroit/Windsor urban air shed, industrial facilities along the shorelines of Lake Huron, Lake St. Clair, and Lake Erie, and regional biogenic VOC sources (largely from Michigan and central and northern Ontario). The proximity of these emissions to the Great Lakes provides the opportunity for the transport and diffusion of pollutant plumes to be modified by the frequent lake- and land-breeze circulations that occur in the summer (e.g., Levy et al., 2010; Makar et al., 2010b).

The goal of this study is first to evaluate the performance of Environment Canada's A Unified Regional Air Quality Modelling System (AURAMS) for predictions of OA in urban and regionally polluted air masses during the BAQS-Met study and then to study the impact that model horizontal grid spacing has on OA concentration predictions.

2 Method description

2.1 Regional air quality modelling system and configuration

Organic aerosol mass concentrations were predicted using version 1.4.0 of AURAMS, which is an off-line regional chemical transport model (CTM) that is driven by the Canadian operational weather forecast model, GEM (Global Environmental Multiscale model) (Côté et al., 1998). Recent descriptions of AURAMS process representations can be found in the following references: chemical boundary conditions in Samaali et al. (2009) and Makar et al. (2010a); gas-phase chemistry and organic speciation in Stroud et al. (2008); biogenic SOA formation in Slowik et al. (2010); dust emissions parameterization in Park et al. (2009); vertical mixing and urban heat island effects in Makar et al. (2006); and cloud processes, aqueous-phase chemistry, and other aspects in Gong et al. (2006).

ACPD
10, 30347–30379, 2010

Hourly anthropogenic point, area, and mobile emissions files were prepared for the AURAMS CTM with the 2005 Canadian and 2005 US national emissions inventories and version 2.3 of the SMOKE emissions processing system (CEP, 2010). Primary organic aerosol (POA) mass emissions were determined from the bulk $PM_{2.5}$ and PM_{10} mass emissions contained in the national inventories through the use of source-specific PM speciation profiles (e.g. mobile, non-mobile, minor point, major point). Biogenic VOC (and NO) emissions were calculated on-line using (1) updated BEIS v3.09 emission factors and algorithms (Schwede et al., 2005), (2) the Biogenic Emissions Landcover Database (BELD3) vegetation data set, and (3) GEM meteorological fields. Emissions for three VOC species were calculated: isoprene; monoterpenes; and "other VOCs". Sesquiterpene emissions are not predicted directly but are calculated as a temperature-dependent function of monoterpene emissions (Helmig et al., 2007). IVOC emissions, which are not accounted for in the standard national emissions inventories, were calculated by multiplying the POA mass emissions by a factor of 1.5, which is calculated assuming that the POA emissions have the volatility basis set (VBS) in Robinson et al. (2007). Emissions in the $C^* = 10^6\ \mu g\,m^{-3}$ and $C^* = 10^5\ \mu g\,m^{-3}$ volatility bins and half of the mass emissions in the $C^* = 10^4\ \mu g\,m^{-3}$ volatility bin are used to derive the factor of 1.5. It is assumed that the remaining half of the mass emissions in the $C^* = 10^4\ \mu g\,m^{-3}$ bin is included in the POA emissions inventory.

The gas-phase chemical mechanism used in this study is an updated version of the ADOM-II mechanism that is solved with the KPP-generated third-order Rosenbrock solver (RODAS3) (Sandu and Sander, 2006). The mechanism VOC speciation was expanded to include a representation for benzene (BENZ) oxidation with the hydroxyl radical (OH). A lumped sesquiterpene species (SESQ) was added to the ADOM-II chemical mechanism and modeled with β-caryophyllene O_3/OH/NO_3 kinetics. Because detailed emissions profiles (i.e., lists of chemical species and their emission proportion by mass for individual source types) do not exist for IVOCs, several assumptions were made to handle this emissions category: (1) IVOC react with an OH oxidation rate coefficient of $3 \times 10^{-11}\ cm^3\ molec^{-1}\ s^{-1}$ (Robinson et al., 2007); and (2) IVOC mass reacts

ACPD
10, 30347–30379, 2010

entirely to form SOA mass (upper limit estimate). A lumped monoterpene species (PINE) was separated from the original ADOM-II long-chain alkene lumped species (ALKE) and assigned the $OH/O_3/NO_3$ kinetics of α-pinene.

A description of the SOA parameterization and references can be found in Slowik et al. (2010). The overall organic aerosol yield approach was applied to the following VOC precursor species: isoprene (ISOP); monoterpenes (PINE); sesquiterpenes (SESQ); benzene (BENZ); mono-substituted aromatics (TOLU); multi-substituted aromatics (AROM); long-chain anthropogenic alkenes (ALKE); and long-chain anthropogenic alkanes (ALKA). SOA yields were calculated for low- and high-NO_x limits as a function of existing organic aerosol loadings (including both primary and secondary aerosol) and temperature (assumed $\Delta H_{vap} = 40\,kJ\,mol^{-1}$) and are based on Raoult's law equilibrium for an ideal solution composed of both POA and SOA. Updated α_i and K_i values are based on recent literature studies: ISOP (Kroll et al., 2006; Lane et al., 2008); PINE (Griffin et al., 1999; Zhang et al., 2006; Pathak et al., 2007); SESQ, ALKE, and ALKA (Lane et al., 2008); BENZ and AROM (Ng et al., 2007); and TOLU (Hildebrandt et al., 2009). A linear interpolation between the low NO_x and high NO_x limits was performed based on the fraction of the RO_2 radicals that react with HO_x vs. NO_x (Presto and Donahue, 2006; Henze et al., 2008).

The AURAMS CTM also incorporates the Canadian Aerosol Module (CAM), which is a size-resolved, multi-component, sectional aerosol parameterization that accounts for nucleation, condensation, coagulation, hygroscopicity and activation, and particle deposition (Gong et al., 2003). Equilibrium inorganic gas-aerosol partitioning was solved with the vectorized HETV module (Makar et al., 2003). Dry deposition of gases is based on Weseley's resistance parameterization. In-cloud aerosol scavenging (aerosol activation to cloud droplets), below-cloud scavenging of gases and particles, evaporation, and in-cloud aqueous chemistry were solved with a cloud processes module (Gong et al., 2006). Currently, the AURAMS CTM considers 12 particle-diameter size bins between 0.01 and 41 µm and nine chemical components (POA, SOA, elemental carbon (EC), sulfate, nitrate, ammonium, sea-salt, crustal material, and particle-bound water).

ACPD
10, 30347–30379, 2010

An organic particle density of 1.5 g cm^{-3} was assumed (Murphy and Pandis, 2009) for conversion of normalized aerosol yield data (from particle volume measurements to mass). Condensation of the SOA to the particle size distribution is described by a modified Fuchs-Sutugin equation (Gong et al., 2003).

A nested grid configuration was used for the AURAMS CTM with an outer continental grid using 42 km horizontal grid spacing, an inner eastern North American grid using 15 km horizontal grid spacing, and a fine-scale 2.5 km grid over the BAQS-Met study region (see Fig. 2 of Makar et al., 2010b). Twenty-eight terrain-following vertical layers were used, with the lowest layer spanning 14 m and the model top located at 29 km a.g.l. AURAMS was run on the 42 km and 15 km grids from 1 June to 15 July 2007 and for the high resolution 2.5 km grid for the period 1 July to 10 July 2007. Climatological chemical lateral boundary conditions (CLBC) are assumed for the 42 km continental domain. Time-dependent CLBC for the 15 km subcontinental domain are provided by the 42 km simulation and time-dependent CLBC for the 2.5 km southern Great Lakes domain are provided by the 15 km simulation. The highest spatial resolution simulation needs to be numerically integrated at finer temporal resolution. The model time step was chosen proportionate to the grid size to maintain numerical stability. For this study, a 900 s time step was used for the 15 km simulation while a 120 s time step was used for the 2.5 km simulation.

2.2 Measurements

Organic aerosol sampling by the University of Toronto (Slowik et al., 2010) during BAQS-Met took place at Harrow, ON from 18 June 2007 to 11 July 2007 and at Bear Creek, ON from 28 June 2007 to 10 July 2007 (see Fig. 5 for locations). Harrow is a rural site surrounded mostly by farmland that is located approximately 40 km southeast of the Detroit/Windsor urban area. Bear Creek is also a rural site surrounded mostly by farmland that is located approximately 60 km northeast of Detroit/Windsor close to the northeast shore of Lake St. Clair. The size-resolved, non-refractory composition

ACPD
10, 30347–30379, 2010

of submicron aerosol particles was measured with an Aerodyne time-of-flight aerosol mass spectrometer (AMS) at both sites.

Organic aerosol sampling with an AMS was also undertaken on two mobile platforms by Environment Canada: CRUISER and the instrumented Convair aircraft (Hayden et al., 2010). CRUISER was stationed for the majority of the campaign in Windsor, but did some daytime excursions eastward to intercept the Detroit/Windsor plume. The aircraft flew out of London, Ontario with some flight tracks over Lake Erie designed to capture the long-range transport of pollutants into the region and some flight tracks focusing on capturing the interaction between the Detroit/Windsor pollutant plume and the Lake St. Clair lake-breeze circulation.

In addition to direct comparisons with the continuous time-of-flight AMS measurements, simulated OA concentration was also 24 h averaged and compared to the observations from the STN (Standard Trends Network) and IMPROVE (Interagency Monitoring of Protected Visual Environments) $PM_{2.5}$ speciation networks, which took 24 h samples every third day between 3 June and 15 July 2007. Samples were collected on quartz filters and analyzed for the $PM_{2.5}$ OC mass concentrations. In 2007 both STN and IMPROVE used the thermo-optical reflectance (TOR) protocol to determine fine organic carbon (OC) concentrations. Factors of 1.4 and 1.8 were used to scale from OC to OA for the STN and IMPROVE networks, respectively, as suggested by Yu et al. (2004) to account for the relative age of the samples. 41 STN sites and 34 IMPROVE sites were considered over eastern North America on the 15 km grid.

3 Results

3.1 Model evaluation statistics

Figure 1 presents a scatterplot comparing AURAMS predicted 24 h $PM_{2.5}$ OA concentration with STN measured 24 h $PM_{2.5}$ OA concentration for the AURAMS simulation at 15 km grid spacing. A factor of 1.4 was used to scale the measured OC to measured

ACPD
10, 30347–30379, 2010

OA since most STN stations are sited in urban locations where fresh POA emissions are expected to dominate (Turpin and Lim, 2001). Table 1 lists the corresponding evaluation statistics for the comparison with the daily STN data. The mean ±standard deviation of the STN OA measurements for all eastern sites for the BAQS-Met period was $6.4 \pm 2.7\,\mu g\,m^{-3}$, which resulted in a mean model bias of $-1.7\,\mu g\,m^{-3}$ and a root mean square error (RMSE) of $3.2\,\mu g\,m^{-3}$. This is a significant improvement in mean bias compared to prior order-of-magnitude OA under-predictions (e.g., McKeen et al., 2007; Smyth et al., 2009; Gong et al., 2010b), which were based on earlier OA yield data from traditional SOA precursors (Odum et al., 1996), lower monoterpene SOA yields (previously lumped monoterpenes and anthropogenic alkenes together), and no ISOP SOA, IVOC SOA or SESQ SOA production. Other recent regional AQ modelling evaluations have also observed a significant improvement in mean bias based on updated OA yield parameters and the introduction of missing SOA precursors such as evaporated SVOCs and IVOCs (Lane et al., 2008; Murphy and Pandis, 2009). The correlation coefficient, R, in Table 1 is 0.51, which is comparable to correlations reported for other predicted secondary aerosol components (e.g., sulfate aerosol) over eastern North America (Gong et al., 2010a). Note that Makar et al. (2010b) showed that $PM_{2.5}$ model-measurement correlation during BAQS-Met is strongly impacted by the ability of the meteorological model to simulate transport and mixing processes. The slope and y-intercept of the best-fit line in Fig. 1 are 0.53 and $1.4\,\mu g\,m^{-3}$, respectively.

Figure 2 shows the corresponding comparison of AURAMS predicted 24 h $PM_{2.5}$ OA concentrations with IMPROVE measurements. The IMPROVE sites are more rural in nature, which results in the sampling of more aged aerosol with higher oxygen-to-carbon composition, so a factor of 1.8 was used to scale from measured OC to measured OA (Turpin and Lim, 2001). Table 1 lists the evaluation statistics for this comparison. The mean ±standard deviation of the IMPROVE 24 h measurements for all eastern sites for the BAQS-Met period was $1.9 \pm 1.4\,\mu g\,m^{-3}$. For this comparison the model actually overpredicts, with a mean bias of $+0.91\,\mu g\,m^{-3}$ and a RMSE of $2.3\,\mu g\,m^{-3}$. The slope and y-intercept of the best-fit line in Fig. 2 are 0.69 and $1.5\,\mu g\,m^{-3}$, respectively.

ACPD
10, 30347–30379, 2010

These results are consistent with another recent AURAMS evaluation study where $PM_{2.5}$ was compared for the 2004 International Consortium for Atmospheric Research on Transport and Transformation (ICARTT) and 2007 BAQS-Met field-study periods. The summer of 2007 was considerably warmer with higher photosynthetically active radiation than 2004, and the modeled SOA was also higher in the summer of 2007 due to increased biogenic emissions. However, the observed $PM_{2.5}$ did not follow the change in temperature and radiation trend and was relatively constant between the two summers (Gong et al., 2010b). These results are consistent with the positive OA bias for the rural IMPROVE sites and suggest the model is over-predicting the biogenic SOA contribution but not the anthropogenic component. A small positive bias was also reported recently for rural sites in the north-eastern US with the volatility-basis-set (VBS) parameterization in the $PMCAM_x$ model (Lane et al., 2008).

Table 2 summarizes the comparison between AURAMS $PM_{2.5}$ OA (15 km grid spacing) with continuous AMS data from the BAQS-Met supersites at Harrow and Bear Creek. Both are rural sites but both are still in close proximity to major urban centres and major point sources). The modelled averages (3.8 and 4.0 $\mu g\,m^{-3}$) for the two sites are quite similar as are the measured averages (6.5 and 7.1 $\mu g\,m^{-3}$). Interestingly, the measured average at the Windsor urban site (7.6 $\mu g\,m^{-3}$) is quite similar to those for Harrow and Bear Creek, which suggests that the Bear Creek and Harrow sites might be better classified as sub-urban rather than rural. As shown in Table 2, AURAMS under-predicts OA for all three locations. The y-intercepts for all comparisons in Table 2 are between 1.3 and 2.0 $\mu g\,m^{-3}$ while the slopes are between 0.28 and 0.42. The RMSE values are also similar for all three BAQS-Met sites and the STN statistics (3.2–4.8 $\mu g\,m^{-3}$). The correlation coefficient is similar for all three sites in Table 2. The correlation coefficients may be higher for the supersites compared to the STN and IMPROVE sites because the AMS measurements at the supersites have higher temporal resolution and can capture the diurnal trend as well as synoptic fluctuations. Alternately, the lower *R* values for the STN and IMPROVE comparisons may indicate that the model's ability to simulate SOA varies with spatial scale, the BAQS-Met domain

ACPD
10, 30347–30379, 2010

being a sub-portion of the model domain where the OA simulations are more accurate than the larger spatial domain.

Table 3 summarizes the high-resolution model comparison with the BAQS-Met aircraft OA concentration data. Due to the computational expense, the focus of the high-resolution model simulations was a shorter period (3–8 July 2007) during which the study area encountered higher OA concentrations. The aircraft OA measurement average was considerably lower than the surface site measurement averages. The modelled aircraft OA average was also lower than the modelled averages for the surface sites; however, the modelled concentrations were closer between the aircraft and the ground sites. In terms of evaluation statistics, the modelled results along the set of aircraft flight tracks resulted in a model positive bias of $+1.3\,\mu g\,m^{-3}$ relative to the aircraft measurements. The y-intercept for the model-aircraft comparison was similar to the model y-intercepts for the surface sites. The best-fit-line slope for the model-aircraft comparison was larger than the slopes for the surface supersites and closer to the IMPROVE correlation slope, which may stem from the aircraft sampling more biogenic-influenced air masses, similar to the composition of the IMPROVE rural sites. The RMSE for the model-aircraft comparison was lower than the RMSEs for the surface supersites. Lastly, the correlation coefficient for the model-aircraft comparison was lower than for the surface sites and likely reflects a spatial correlation more than a diurnal correlation (most flights were during daytime).

3.2 Impact of grid spacing on modelled organic aerosol time series

Figure 3a illustrates the impact of model grid spacing for time series of observed and model-predicted OA for 3–7 June at the Bear Creek site. The simulation for 42 km grid spacing results in a time series that is consistently lower than those for the other two higher-resolution simulations. In comparing the 15 km and 2.5 km simulation time series, both simulations capture temporal variations in the regional background whereas the 2.5 km simulation better captures the higher concentration peaks.

ACPD
10, 30347–30379, 2010

The model concentration-frequency histogram for Bear Creek shown in Fig. 4 illustrates the improvement in the high-concentration "tail" region associated with the highest-resolution simulation. The 15 km simulation average for the 3–8 July 2007 period is 4.9 $\mu g\,m^{-3}$ compared to a measured average of 7.9 $\mu g\,m^{-3}$ and an average of 5.3 $\mu g\,m^{-3}$ for the high-resolution 2.5 km simulation. However, there is little change in correlation coefficient between the two simulations: $R = 0.72$ for the 15 km simulation vs. $R = 0.68$ for the 2.5 km simulation. This result reflects the difficulty in capturing *both* the spatial location and temporal variation for narrow plumes, for which only small shifts in location or time can cause an anti-correlation, whereas the 15 km grid spacing is more forgiving to near-misses.

Figure 3b and c illustrate the impact of model grid spacing for Harrow and Windsor, respectively. In general, the same conclusions can be drawn. For Harrow, the 15 km resolution model average for the 3–8 July 2007 period is 5.2 $\mu g\,m^{-3}$ compared to a measured average of 10.8 $\mu g\,m^{-3}$ and an average of 5.8 $\mu g\,m^{-3}$ for the high-resolution 2.5 km simulation. However, there is again little change in correlation coefficient in comparing the 15 km and 2.5 km simulations: $R = 0.68$ vs. $R = 0.64$. For Windsor, the 15 km simulation average for the 3–8 July 2007 period is 7.3 $\mu g\,m^{-3}$ compared to a measured average of 8.9 $\mu g\,m^{-3}$ and an average of 8.2 $\mu g\,m^{-3}$ for the high-resolution 2.5 km simulation. There is a slightly larger change in correlation coefficient for Windsor between the 15 km and 2.5 km simulations: $R = 0.68$ vs. $R = 0.60$. Again this likely reflects the difficulty in capturing fine-scale features in space and time.

For all three stations the predicted time series of OA mass concentration for the 42 km simulation shown in Fig. 3 are consistently smaller than those for the two higher-resolution simulations. The 15 km run captures the regional background adequately but the highest-resolution 2.5 km run better captures the frequency and amplitude of OA maxima (e.g., histograms in Fig. 4). The need for high-resolution modelling for urban airsheds is illustrated in Fig. 4 by the improvement in the concentration-frequency histogram for Windsor in going from 42 km to 15 km to 2.5 km grid spacing.

ACPD
10, 30347–30379, 2010

3.3 Impact of grid spacing on spatial distribution of organic aerosol

Figure 5 compares the time-averaged spatial distributions of ground-level $PM_{2.5}$ OA for the 15 km and 2.5 km simulations for the period 4 July, 00:00 Z to 10 July, 00:00 Z. The average $PM_{2.5}$ OA surface mass concentration over the entire 2.5 km domain is $4.8 \pm 0.7\,\mu g\,m^{-3}$ while the average $PM_{2.5}$ OA mass concentration for the windowed 15 km domain corresponding to the 2.5 km domain is $4.3 \pm 0.7\,\mu g\,m^{-3}$. Both simulations result in similar OA mass concentrations for regional background grid cells (e.g., over Lake Huron). However, the higher-resolution model simulation predicts considerably higher maximum grid-cell $PM_{2.5}$ OA mass concentration by a factor of seven ($6.9\,\mu g\,m^{-3}$ for the 15 km run vs. $50\,\mu g\,m^{-3}$ for the 2.5 km run).

Figures 6 and 7 compare the time-averaged spatial distributions of POA and SOA from the 15 km and 2.5 km simulations for the same period. The average $PM_{2.5}$ POA surface mass concentration over the 2.5 km domain is $0.48 \pm 0.4\,\mu g\,m^{-3}$ vs. $0.46 \pm 0.3\,\mu g\,m^{-3}$ for the windowed 15 km surface plot. However, the higher-resolution model run predicts a much higher maximum grid cell $PM_{2.5}$ POA mass concentration by a factor of 15 (2.4 vs. $36\,\mu g\,m^{-3}$).

The time-averaged spatial distributions of $PM_{2.5}$ SOA shown in Fig. 7 are more uniform spatially than the $PM_{2.5}$ POA distributions since SOA formation occurs on regional scales. The average $PM_{2.5}$ SOA surface mass concentration over the 2.5 km domain is $4.3 \pm 0.4\,\mu g\,m^{-3}$ vs. $3.9 \pm 0.4\,\mu g\,m^{-3}$ for the windowed 15 km surface plot (9% increase), but the higher-resolution model run predicts a higher maximum grid cell $PM_{2.5}$ SOA mass concentration by a factor of 3 (5.1 vs. $15\,\mu g\,m^{-3}$).

ACPD
10, 30347–30379, 2010

4 Discussion

The increase in OA mass concentrations at higher resolutions could be due to several factors: (1) spatial variations in POA emissions are better represented for urban and industrial sources with finer-resolution grids; (2) meteorological features such as pollutant maxima along lake-breeze fronts are better resolved; (3) SOA formation chemistry depends on precursor VOC and oxidant levels, which have their own non-linear dependencies (i.e., precursor VOC levels depend on emissions their spatial resolution while oxidant levels depend on VOC levels, NO_x levels, and VOC/NO_x ratios); and (4) the SOA partitioning process depends non-linearly on pre-existing OA mass concentrations. This last factor implies that better spatial resolution of the POA emissions may have an additional feedback on the SOA yields.

The model performance evaluation statistics in Sect. 3.3 show that the maximum grid-cell $PM_{2.5}$ OA concentration change resulting from different grid spacing is greater for the POA component than the SOA component. This suggests that for grid cells with large industrial emissions (e.g., Monroe County, MI) or areas with large urban emission gradients (e.g., Toronto and Detroit plumes), the most important impact of the highest-resolution grid spacing is to better resolve the POA emissions. However, the increase in maximum SOA concentration with higher-resolution grid spacing still makes a significant contribution to the maximum grid-cell $PM_{2.5}$ OA concentration increase from 6.9 to 50 $\mu g\,m^{-3}$. As noted above, the SOA production rates depend on precursor mixing ratios, oxidant levels, and SOA yields. Using the toluene SOA yield data for high NO_x conditions (Ng et al., 2007) as an example, the SOA yield changes from 7% to 13% or a factor of 2 for OA concentrations changing from 6.9 to 50 $\mu g\,m^{-3}$. Oxidant levels for urban air sheds are often VOC-limited or near the transition from VOC-limited to NO_x-limited conditions. In general, on a relative scale, OH and O_3 concentrations change less in going from urban to sub-urban locations than do precursor VOC concentrations. Similar to the POA emissions, higher-resolution grid spacing is likely to be more important for the representation of VOC emissions and hence VOC concentrations as

ACPD
10, 30347–30379, 2010

compared to the representation of oxidant levels or SOA yields. Finer-scale meteorology likely also plays a role in better capturing fine-scale OA concentration features of a more episodic nature. A companion paper uses the high-resolution AURAMS model to illustrate, through a series of case studies, the enhancement of predicted OA along convergence zones associated with lake-breeze fronts (Stroud et al., 2010).

5 Conclusions

We performed predictions of $PM_{2.5}$ OA with Environment Canada's AURAMS air-quality modelling system for summer 2007 for a nested grid configuration spanning continental-to-regional-to-urban scales. Model-measurement comparisons were made with STN and IMPROVE network data and the BAQS-Met supersite data for the regional-scale eastern North American domain at 15 km grid spacing. These extended time series comparisons (3 June–15 July 2007) resulted in model underpredictions of $PM_{2.5}$ OA vs. the STN measurements (MB of $-1.7\,\mu g\,m^{-3}$) and BAQS-Met measurements (MB of -2.4 to $-3.1\,\mu g\,m^{-3}$) and overpredictions vs. the IMPROVE measurements (MB of $0.91\,\mu g\,m^{-3}$). These results suggest that the model is overpredicting biogenic SOA formation and underpredicting anthropogenic SOA formation. The evaluation against one-day-in-three 24 h network OA measurements yielded correlation coefficients of 0.43 to 0.51 (largely synoptic spatial and time scales, excludes diurnal and shorter time scales) whereas evaluation with the continuous BAQS-Met OA measurements yielded correlation coefficients of 0.60 to 0.72 (largely temporal, including diurnal, variations). High-resolution model-measurement comparisons with aircraft OA data (2.5 km grid spacing with extractions along flight tracks) yielded a MB of $+1.3\,\mu g\,m^{-3}$ and a correlation coefficient of 0.51 (largely mesoscale spatial variations).

In general, for the BAQS-Met supersites, the 42 km continental-scale results were consistently biased low relative to the 15 km regional scale results. The 15 km and 2.5 km simulations yielded similar $PM_{2.5}$ OA mass concentrations for regional-scale and longer-term averages (within 9% for 15 km windowed domain average

ACPD
10, 30347–30379, 2010

comparison with 2.5 km domain). However, the 2.5 km simulation yielded a model concentration-frequency histogram for the Windsor urban site in better agreement with the measurement-based histogram compared to the 42 km and 15 km simulations. The model histograms for Bear Creek and Harrow were also improved in the high-concentration "tail" region, and the highest-resolution run captured the midday 4 July urban plume at Bear Creek with very good temporal correlation. Clearly, for urban and large industrial plumes, the highest spatial resolution is needed to capture spatial gradients in urban POA emissions, precursor VOC emissions, and SOA production rate. The positive feedback between SOA production rate and existing organic mass concentration is best represented with the highest spatial resolution. Overall, inadequate model grid spacing is very likely an additional factor contributing to model underprediction of urban OA measurements as reported in the literature.

Acknowledgements. The authors are grateful to the sponsors and administrators of the IMPROVE and STN networks for providing long-term aerosol composition measurements. The authors are also grateful to the Pollution Data Division of Environment Canada for emission inventory compilation and to the Canadian Meteorological Centre for development of GEM and for emissions processing support. Lastly, the authors acknowledge Environment Canada and the Ontario Ministry of the Environment for funding the BAQS-Met study.

References

Carlton, A. G., Turpin, B. J., Altieri, K. E., Seitzinger, S. P., Mathur, R., Roselle, S. J., and Weber, R. J.: CMAQ model performance enhanced when in-cloud secondary organic aerosol is included: Comparisons of organic carbon predictions with measurements, Environ. Sci. Technol., 42(23), 8798–8802, 2008.

CEP (Carolina Environmental Program): Sparse Matrix Operator Kernel Emission (SMOKE) modelling system, available at: http://www.smoke-model.org/index.cfm, University of North Carolina, Chapel Hill, North Carolina, 2010.

Chen, J., Mao, H., Talbot, R. W., and Griffin, R. J.: Application of the CACM and MPMPO

ACPD

10, 30347–30379, 2010

modules using the CMAQ model for the eastern United States, J. Geophys. Res., 111(23), D23S25, D23S25, 2006.
Cohan, D. S., Hu, Y., and Russell, A. G.: Dependence of ozone sensitivity analysis on grid resolution, Atmos. Environ., 40, 126–135, 2006.
Gillani, N. V. and Pleim, J. E.: Sub-grid-scale features of anthropogenic emissions of NO_x and VOC in the context of regional Eulerian models, Atmos. Environ., 30, 2043–2059, 1996.
Côté, J., Gravel, S., Méthot, A., Patoine, A., Roch, M., and Staniforth, A.: The operational CMC-MRB global environmental multiscale (GEM) model, Part I: Design considerations and formulation. Mon. Weather Rev., 126, 1373–1395, 1998.
Davidson, C. I., Phalen, R. F., and Solomon, P. A.: Airborne particulate matter and human health: A review, Aerosol Sci. Technol., 39, 737–749, 2005.
Goldstein, A. H. and Galbally, I. E.: Known and unexplored organic constituents in the earth's atmosphere, Environ. Sci. Technol., 41(5), 1514–1521, 2007.
Gong, S. L., Barrie, L. A., Blanchet, J.-P., von Salzen, K., Lohmann, U., Lesins, G., Spacek, L., Zhang, L. M., Girard, E., Lin, H., Leaitch, R., Leighton, H., Chylek, P. and Huang, P.: Canadian Aerosol Module: A size segregated simulation of atmospheric aerosol processes for climate and air quality models: Part 1. Module development, J. Geophys. Res., 108(D1), 16 pp., 4007, doi:10.1029/2001JD002002, 2003.
Gong, W., Dastoor, A. P., Bouchet, V. S., Gong, S., Makar, P. A., Moran, M. D., Pabla, B., Ménard, S., Crevier, L.-P., Cousineau, S., and Venkatesh, S.: Cloud processing of gases and aerosols in a regional air quality model (AURAMS), Atmos. Res., 82, 248–275, 2006.
Gong, W., Farrell, C., Makar, P. A., Menard, R., Michael, D., Moran, M. D., Morneau, G., and Stroud, C.: Canadian smog science assessment, Chapter 6: Model description and evaluation, 2010a.
Gong, W., Zhang, J., Makar, P. A., Moran, M. D., Stroud, C., Gravel, S., Gong, S., and Pabla, B.: Comparative evaluation of model simulations of regional ozone and particulate matters for two distinct summers over eastern North America, Proc. 31st NATO/SPS Intern. Tech. Mtg on Air Pollution Modelling and Its Application, 27 Sept.–1 Oct., Turin, 2010b.
Griffin, R. J., Cocker III, D. R., Flagan, R. C., and Seinfeld, J. H.: Organic aerosol formation from the oxidation of biogenic hydrocarbons, J. Geophys. Res., 104, 3555–3567, 1999.
Griffin, R. J., Dabdub, D., and Seinfeld, J. H.: Development and initial evaluation of a dynamic species-resolved model for gas phase chemistry and size-resolved gas/particle partitioning associated with secondary organic aerosol formation, J. Geophys. Res, 110(5), 1–16, 2005.

ACPD
10, 30347–30379, 2010

Hallquist, M., Wenger, J. C., Baltensperger, U., Rudich, Y., Simpson, D., Claeys, M., Dommen, J., Donahue, N. M., George, C., Goldstein, A. H., Hamilton, J. F., Herrmann, H., Hoffmann, T., Iinuma, Y., Jang, M., Jenkin, M. E., Jimenez, J. L., Kiendler-Scharr, A., Maenhaut, W., McFiggans, G., Mentel, Th. F., Monod, A., Prèvôt, A. S. H., Seinfeld, J. H., Surratt, J. D., Szmigielski, R., and Wildt, J.: The formation, properties and impact of secondary organic aerosol: current and emerging issues, Atmos. Chem. Phys., 9, 5155–5236, doi:10.5194/acp-9-5155-2009, 2009.

Hayden, K. L., Sills, D. M. L., Brook, J. R., Li, S.-M., Markovic, M., Liu, P., Anlauf, K. G., O'Brien, J. M., Strawbridge, K., Firanski, B., and McLaren, R.: The impact of lake breezes on trace gases and particles during the Border Air Quality and Meteorology Study (BAQS-Met), Atmos. Chem. Phys. Discuss., submitted, 2010.

Heald, C. L., Jacob, D. J., Park, R. J., Russell, L. M., Huebert, B. J., Seinfeld, J. H., Liao, H., and Weber, R. J.: A large organic aerosol source in the free troposphere missing from current models, Geophys. Res. Lett., 32(18), 1–4, L18809, doi:10.1029/2005GL023831, 2005.

Helmig, D., Ortega, J., Duhl, T., Tanner, D., Guenther, A., Harley, P., Wiedinmyer, C., Milford, J., and Sakulyanontvittaya, T.: Sesquiterpene emissions from pine trees – identifications, emission rates and flux estimates for the contiguous United States, Environ. Sci. Technol., 41, 1545–1553, 2007.

Henze, D. K., Seinfeld, J. H., Ng, N. L., Kroll, J. H., Fu, T.-M., Jacob, D. J., and Heald, C. L.: Global modeling of secondary organic aerosol formation from aromatic hydrocarbons: high- vs. low-yield pathways, Atmos. Chem. Phys., 8, 2405–2420, doi:10.5194/acp-8-2405-2008, 2008.

Hildebrandt, L., Donahue, N. M., and Pandis, S. N.: High formation of secondary organic aerosol from the photo-oxidation of toluene, Atmos. Chem. Phys., 9, 2973–2986, doi:10.5194/acp-9-2973-2009, 2009.

Jang, J.-C. C., Jeffries, H. E., Byun, D., and Pleim, J. E.: Sensitivity of ozone to model grid resolution. Part I. Application of high-resolution Regional Acid Deposition Model, Atmos. Environ., 29, 3085–3100, 1995a.

Jang, J.-C. C., Jeffries, H. E., and Tonnesen, S.: Sensitivity of ozone to model grid resolution. Part II. Detailed process analysis for ozone chemistry, Atmos. Environ., 29, 3101–3114, 1995b.

Karamchandani, P., Seigneur, C., Vijayaraghavan, K., and Wu, S.-Y.: Development and application of a state-of-the-science plume-in-grid model, J. Geophys. Res., 107, 13 pp., 4403,

ACPD
10, 30347–30379, 2010

doi:10.1029/2002JD002123, 2002.
Karamchandani, P., Vijayaraghavan, K., Chen, S.-Y., Seigneur, C., and Edgerton, E. S.: Plume-in-grid modeling for particulate matter, Atmos. Environ., 40, 7280–7297, 2006.
Kroll, J. H., Ng, N. L., Murphy, S. M., Flagan, R. C., and Seinfeld, J .H.: Secondary aerosol formation from isoprene photooxidaation, Environ. Sci. Technol., 40, 1869–1877, 2006.
Lane, T. E., Donahue, N. M., and Pandis, S. N:. Effect of NO_x on secondary organic aerosol concentrations, Environ. Sci. Technol., 42, 6022–6027, 2008.
Levy, I., Makar, P. A., Sills, D., Zhang, J., Hayden, K. L., Mihele, C., Narayan, J., Moran, M. D., Sjostedt, S., and Brook, J.: Unraveling the complex local-scale flows influencing ozone patterns in the southern Great Lakes of North America, Atmos. Chem. Phys., 10, 10895–10915, doi:10.5194/acp-10-10895-2010, 2010.
Makar, P. A., Bouchet, V. S., and Nenes, A.: Inorganic chemistry calculations using HETV – a vectorized solver for the SO_4^{2-}–NO_3^-–NH_4^+ system based on the ISORROPIA algorithms, Atmos. Environ., 37, 2279–2294, 2003.
Makar, P. A., Gravel, S., Chirkov, V., Strawbridge, K. B., Froude, F., Arnold, J., and Brook, J.: Heat flux, urban properties, and regional weather, Atmos. Environ., 40, 2750–2766, 2006.
Makar, P. A., Gong, W., Mooney, C., Zhang, J., Davignon, D., Samaali, M., Moran, M. D., He, H., Tarasick, D. W., Sills, D., and Chen, J.: Dynamic adjustment of climatological ozone boundary conditions for air-quality forecasts, Atmos. Chem. Phys., 10, 8997–9015, doi:10.5194/acp-10-8997-2010, 2010a.
Makar, P. A., Zhang, J., Gong, W., Stroud, C., Sills, D., Hayden, K. L., Brook, J., Levy, I., Mihele, C., Moran, M. D., Tarasick, D. W., He, H., and Plummer, D.: Mass tracking for chemical analysis: the causes of ozone formation in southern Ontario during BAQS-Met 2007, Atmos. Chem. Phys., 10, 11151–11173, doi:10.5194/acp-10-11151-2010, 2010.
McKeen, S., Chung, S. H., Wilczak, J., Grell, G., Djalalova, I., Peckham, S., Gong, W., Bouchet, V., Moffet, R., Tang, Y., Carmichael, G. R., Mathur, R., and Yu, S.: Evaluation of several real-time $PM_{2.5}$ forecast models using data collected during the ICARTT/NEAQS 2004 field study, J. Geophys. Res., 112, 20 pp., D10S20, doi:10.1029/2006JD007608, 2007.
Murphy, B. N. and Pandis, S. N.: Simulating the formation of semivolatile primary and secondary organic aerosol in a regional chemical transport model, Environ. Sci. Technol., 43(13), 4722–4728, 2009.
Ng, N. L., Kroll, J. H., Chan, A. W. H., Chhabra, P. S., Flagan, R. C., and Seinfeld, J. H.: Secondary organic aerosol formation from m-xylene, toluene, and benzene, Atmos. Chem.

ACPD
10, 30347–30379, 2010

Phys., 7, 3909–3922, doi:10.5194/acp-7-3909-2007, 2007.
Odum, J. R., Jungkamp, T. P. W., Griffin, R. J., Flagan, R. C., and Seinfeld, J. H.: The atmospheric aerosol-forming potential of whole gasoline vapour, Science, 276(5309), 96–99, 1997.
Pagowski, M., Grell, G. A., McKeen, S. A., Dévényi, D., Wilczak, J. M., Bouchet, V., Gong, W., McHenry, J., Peckham, S., McQueen, J., Moffet, R., and Tang, Y.: A simple method to improve ensemble-based ozone forecasts, Geophys. Res. Lett., 32, L07814, 4 pp., doi:10.1029/2004GL022305, 2005.
Park, S. H., Gong, S. L., Gong, W., Makar, P. A., Moran, M. D., Stroud, C. A., and Zhang, J.: Sensitivity of surface characteristics on the simulation of wind-blown-dust source in North America, Atmos. Environ., 43(19), 3122–3129, 2009.
Pathak, R. K., Presto, A. A., Lane, T. E., Stanier, C. O., Donahue, N. M., and Pandis, S. N.: Ozonolysis of α-pinene: parameterization of secondary organic aerosol mass fraction, Atmos. Chem. Phys., 7, 3811–3821, doi:10.5194/acp-7-3811-2007, 2007.
Presto, A. A. and Donahue, N. M.: Investigation of α-pinene + ozone secondary organic aerosol formation at low total aerosol mass, Environ. Sci. Technol., 40, 3536–3543, 2006.
Robinson, A. L., Donahue, N. M., Shrivastava, M. K., Weitkamp, E. A., Sage, A. M., Grieshop, A. P., Lane, T. E., Pierce, J. R., and Pandis, S. N.: Rethinking organic aerosols: Semivolatile emissions and photochemical aging, Science, 315(5816), 1259–1262, 2007.
Samaali, M., Moran, M. D., Bouchet, V. S., Pavlovic, R., Cousineau, S., and Sassi, M.: On the influence of chemical initial and boundary conditions on annual regional air quality model simulations for North America, Atmos. Environ., 43, 4873–4885, 2009.
Sandu, A. and Sander, R.: Technical note: Simulating chemical systems in Fortran90 and Matlab with the Kinetic PreProcessor KPP-2.1, Atmos. Chem. Phys., 6, 187–195, doi:10.5194/acp-6-187-2006, 2006.
Schwede, D., Pouliot, G., and Pierce, T.: Changes to the biogenic emissions inventory system version 3, CMAS Extended Abstract, 2005.
Slowik, J. G., Stroud, C., Bottenheim, J. W., Brickell, P. C., Chang, R. Y.-W., Liggio, J., Makar, P. A., Martin, R. V., Moran, M. D., Shantz, N. C., Sjostedt, S. J., van Donkelaar, A., Vlasenko, A., Wiebe, H. A., Xia, A. G., Zhang, J., Leaitch, W. R., and Abbatt, J. P. D.: Characterization of a large biogenic secondary organic aerosol event from eastern Canadian forests, Atmos. Chem. Phys., 10, 2825–2845, doi:10.5194/acp-10-2825-2010, 2010.
Smyth, S. C., Jiang, W., Roth, H., Moran, M. D., Makar, P. A., Yang, F., Bouchet, V. S., and

ACPD
10, 30347–30379, 2010

Landry, H.: A comparative performance evaluation of the AURAMS and CMAQ air quality modelling systems, Atmos. Environ., 43, 1059–1070, 2009.
Stroud, C. A., Morneau, G., Makar, P. A., Moran, M. D., Gong, W., Pabla, B., Zhang, J., Bouchet, V. S., Fox, D., Venkatesh, S., Wang, D., and Dann, T.: OH-reactivity of volatile organic compounds at urban and rural sites across Canada: Evaluation of air quality model predictions using speciated VOC measurements, Atmos. Environ., 42, 7746–7756, 2008.
Stroud, C. A., Abbatt, J., Slowik, J., Makar, P. A., Moran, M. D., Gong, W., Gong, S., Zhang, J., Mihele, C., Lu, G., Brook, J. R., Liu, P., Sills, D., and Li, Q.: Characterization of primary and secondary organic aerosol in southern Ontario using high-resolution chemical transport modelling and receptor-based positive matrix factorization methods, Atmos. Chem. Phys. Discuss., in preparation, 2010.
Tsimpidi, A. P., Karydis, V. A., Zavala, M., Lei, W., Molina, L., Ulbrich, I. M., Jimenez, J. L., and Pandis, S. N.: Evaluation of the volatility basis-set approach for the simulation of organic aerosol formation in the Mexico City metropolitan area, Atmos. Chem. Phys., 10, 525–546, doi:10.5194/acp-10-525-2010, 2010.
Turpin, B. J. and Lim, H.-J.: Species contributions to $PM_{2.5}$ mass concentrations: Revisiting common assumptions for estimating organic mass, Aerosol Sci. Technol., 35(1), 602–610, 2001.
Ying, Q., Fraser, M. P., Griffin, R. J., Chen, J., and Kleeman, M. J.: Verification of a source-oriented externally mixed air quality model during a severe photochemical smog episode, Atmos. Environ., 41(7), 1521–1538, 2007.
Yu, S., Dennis, R. L., Bhave, P. V., and Eder, B. K.: Primary and secondary organic aerosols over the United States: Estimates on the basis of observed organic carbon (OC) and elemental carbon (EC), and air quality modeled primary OC/EC ratios, Atmos. Environ., 38(31), 5257–5268, 2004.
Yu, S., Bhave, P. V., Dennis, R. L., and Mathur, R.: Seasonal and regional variations of primary and secondary organic aerosols over the continental United States: Semi-empirical estimates and model evaluation, Environ. Sci. Technol., 41(13), 4690–4697, 2007.
Zhang, J., Huff, Hartz, K. E., Pandis, S. N., and Donahue, N. M.: Secondary organic aerosol formation from limonene ozonolysis: Homogeneous and heterogeneous influences as a function of NO_x, J. Phys. Chem. A, 110, 11053–11063, 2006.
Zhang, Q., Jimenez, J. L., Canagaratna, M. R., Allan, J. D., Coe, H., Ulbrich, I., Alfarra, M. R., Takami, A., Middlebrook, A. M., Sun, Y. L., Dzepina, K., Dunlea, E., Docherty, K., De-

ACPD
10, 30347–30379, 2010

Carlo, P. F., Salcedo, D., Onasch, T., Jayne, J. T., Miyoshi, T., Shimono, A., Hatakeyama, S., Takegawa, N., Kondo, Y., Schneider, J., Drewnick, F., Borrmann, S., Weimer, S., Demerjian, K., Williams, P., Bower, K., Bahreini, R. B., Cottrell, L., Griffin, R. J., Rautiainen, J., Sun, J. Y., Zhang, Y. M., Worsnop, and D. R.: Ubiquity and dominance of oxygenated species in organic aerosols in anthropogenically-influenced northern hemisphere midlatitudes, Geophys. Res. Lett., 34(13), L13801, doi:10.1029/2007GL029979, 2007.

ACPD
10, 30347–30379, 2010

Table 1. Comparison of AURAMS $PM_{2.5}$ OA predictions (15 km grid spacing) with 24 h STN and IMPROVE data for 3 June–15 July 2007 (includes standard deviation of the distribution around the mean).

Statistic	STN	IMPROVE
Number of Points	946	480
Model OA Average ($\mu g\,m^{-3}$)	4.8 ± 2.7	3.5 ± 2.6
Data OA Average ($\mu g\,m^{-3}$)	6.4 ± 2.7	1.9 ± 1.4
Best-fit Line Slope	0.53 ± 0.03	0.69 ± 0.06
Best-fit Line y-Intercept ($\mu g\,m^{-3}$)	1.4 ± 0.2	1.5 ± 0.2
Slope (forced y-intercept to zero)	0.98 ± 0.02	1.20 ± 0.04
Mean Bias ($\mu g\,m^{-3}$)	−1.7	+0.91
RMSE ($\mu g\,m^{-3}$)	3.2	2.3
Correlation, R	0.51	0.43

Assumed an OA to OC ratio of 1.4 (by mass) for STN data and 1.8 (by mass) for IMPROVE data.

ACPD
10, 30347–30379, 2010

Table 2. Comparison of AURAMS $PM_{2.5}$ OA predictions (15 km grid spacing) with 5 min average Harrow and Bear Creek AMS data and 1 min average Windsor CRUISER AMS data (includes standard deviation of the distribution around the mean).

Statistic	Harrow	Bear Creek	Windsor
Number of Data Pairs	4315 (22 June–10 July)	813 (29 June–10 July)	20019 (22 June–10 July)
Model OA Average ($\mu g\,m^{-3}$)	3.8 ± 2.1	4.0 ± 2.5	5.2 ± 2.9
Data OA Average ($\mu g\,m^{-3}$)	6.5 ± 4.9	7.1 ± 4.9	7.6 ± 4.1
Slope	0.28 ± 0.01	0.38 ± 0.01	0.421 ± 0.004
y-Intercept ($\mu g\,m^{-3}$)	1.98 ± 0.04	1.3 ± 0.1	1.97 ± 0.03
Mean Bias ($\mu g\,m^{-3}$)	−2.7	−3.1	−2.4
RMSE ($\mu g\,m^{-3}$)	4.8	4.7	4.1
Correlation, *R*	0.65	0.72	0.60

ACPD
10, 30347–30379, 2010

Table 3. Comparison of AURAMS $PM_{2.5}$ OA predictions (2.5 km grid spacing) with aircraft 2 min average AMS data (includes standard deviation of the distribution around the mean).

Number of Data Pairs	371 (Flights 12–16) (3 July, 7ab, 8ab)
Model OA Average ($\mu g\,m^{-3}$)	5.6 ± 2.6
Data OA Average ($\mu g\,m^{-3}$)	4.2 ± 1.5
Slope	0.87 ± 0.08
Intercept ($\mu g\,m^{-3}$)	1.9 ± 0.3
Mean Bias ($\mu g\,m^{-3}$)	+1.3
RMSE ($\mu g\,m^{-3}$)	2.6
Correlation, *R*	0.51

Total flying time was ~12 h. Most flights were during daylight hours with the exception of 7 July flight 1 (03:36–06:16 EST).

ACPD
10, 30347–30379, 2010

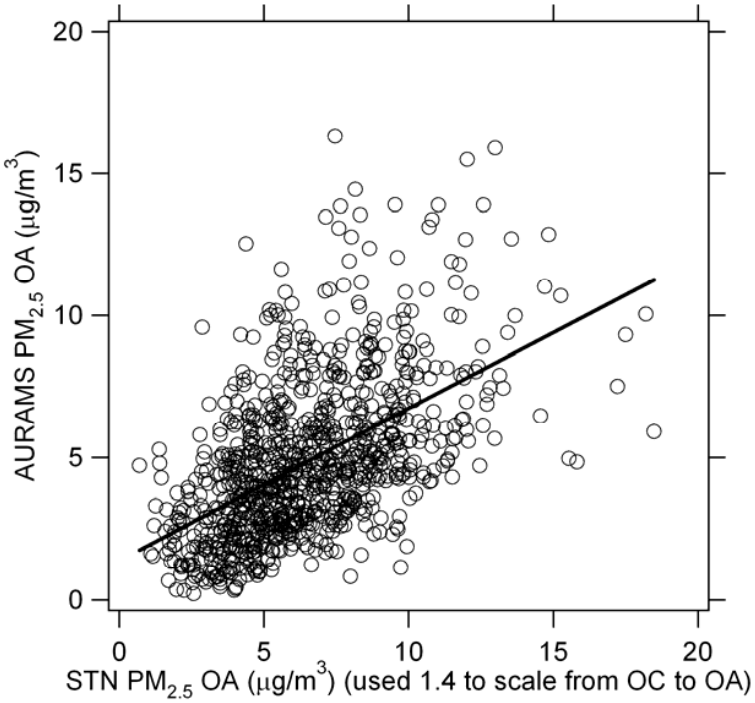

Fig. 1. Scatterplot of AURAMS predicted 24 h $PM_{2.5}$ OA concentration vs. STN measured 24 h $PM_{2.5}$ OA concentration for the 15 km-grid simulation for the period 3 June to 15 July 2007. The least-squares best-fit line is also plotted.

ACPD
10, 30347–30379, 2010

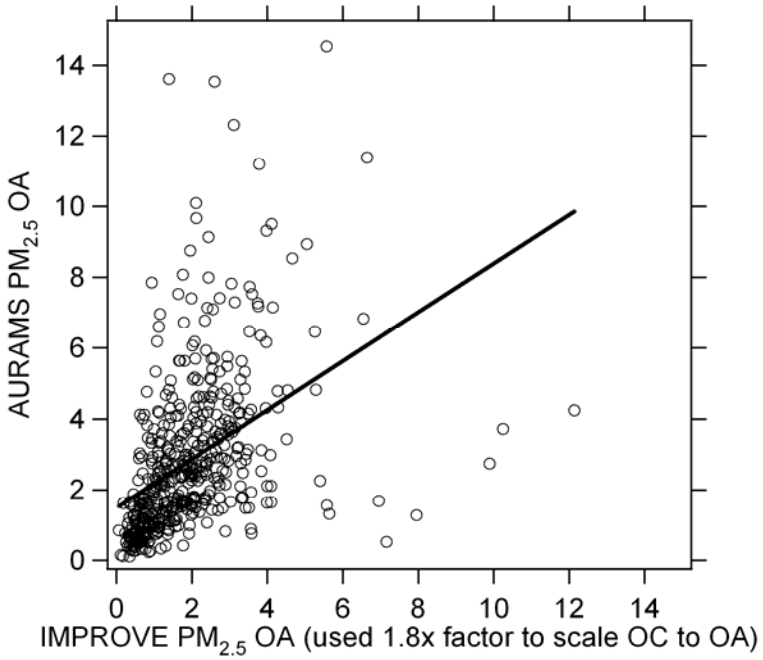

Fig. 2. Same as Fig. 1 but for the IMPROVE network.

ACPD
10, 30347–30379, 2010

Impact of model grid spacing on regional- and urban-scale air quality predictions

C. A. Stroud et al.

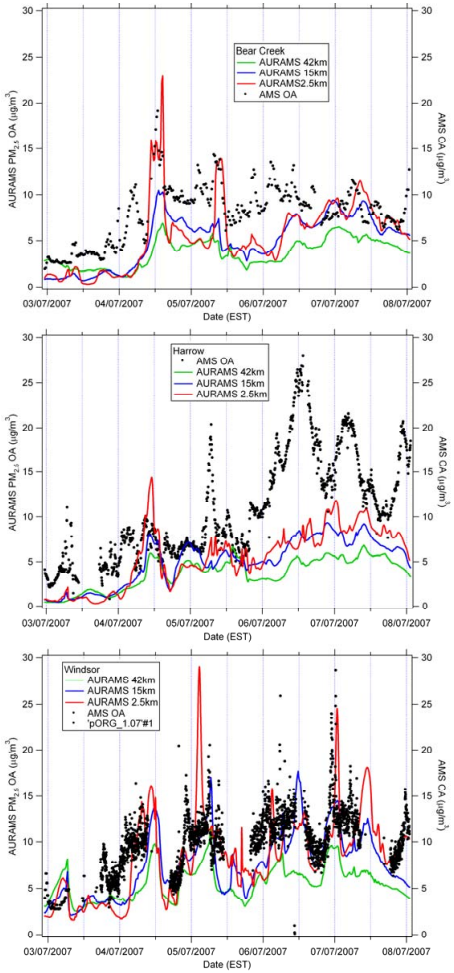

Fig. 3. OA time series comparison for the three different grid-spacing AURAMS simulations (42, 15, and 2.5 km) at Bear Creek, Harrow, and Windsor including the AMS measurement data. In panel B, the AMS data is plotted on the right-hand y-axis.

ACPD
10, 30347–30379, 2010

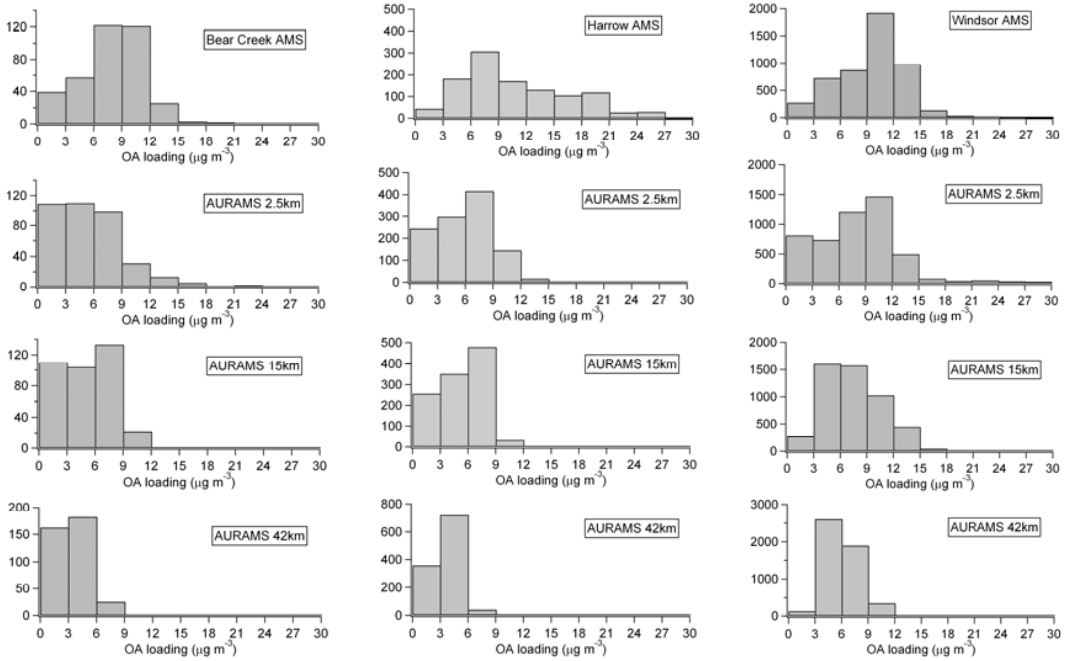

Fig. 4. Histograms (number of samples vs. concentration range) are plotted for measurement data from 3–8 July 2007. Corresponding model data are also included at 42 km, 15 km, and 2.5 km grid spacing for Bear Creek, Harrow, and Windsor.

ACPD
10, 30347–30379, 2010

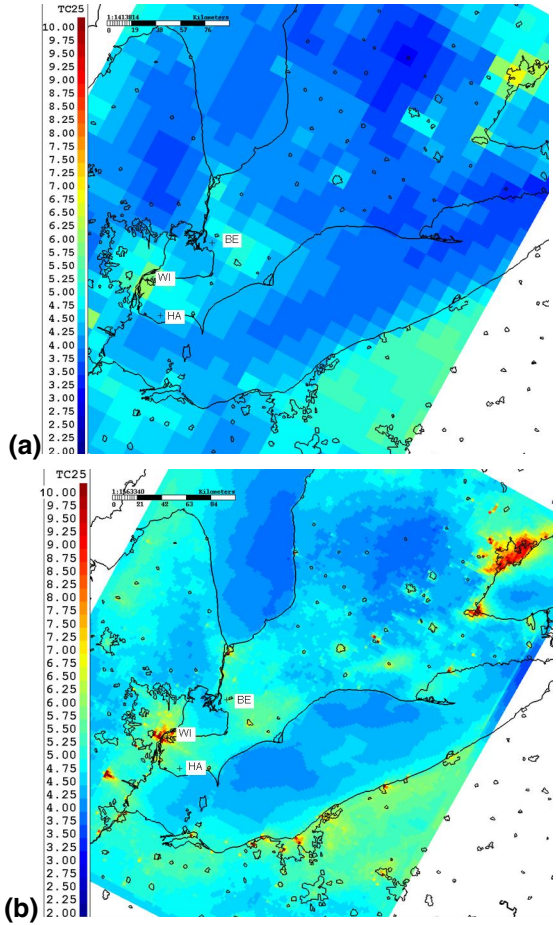

Fig. 5. Time-averaged model $PM_{2.5}$ OA concentration results ($\mu g\,m^{-3}$) for **(a)** the windowed 15 km grid and **(b)** the full 2.5 km grid (4 July, 00:00 Z to 10 July, 00:00 Z). Plus signs mark the locations of the Bear Creek ("BE"), Harrow ("HA"), and Windsor ("WI") monitoring sites.

ACPD
10, 30347–30379, 2010

Impact of model grid spacing on regional- and urban-scale air quality predictions

C. A. Stroud et al.

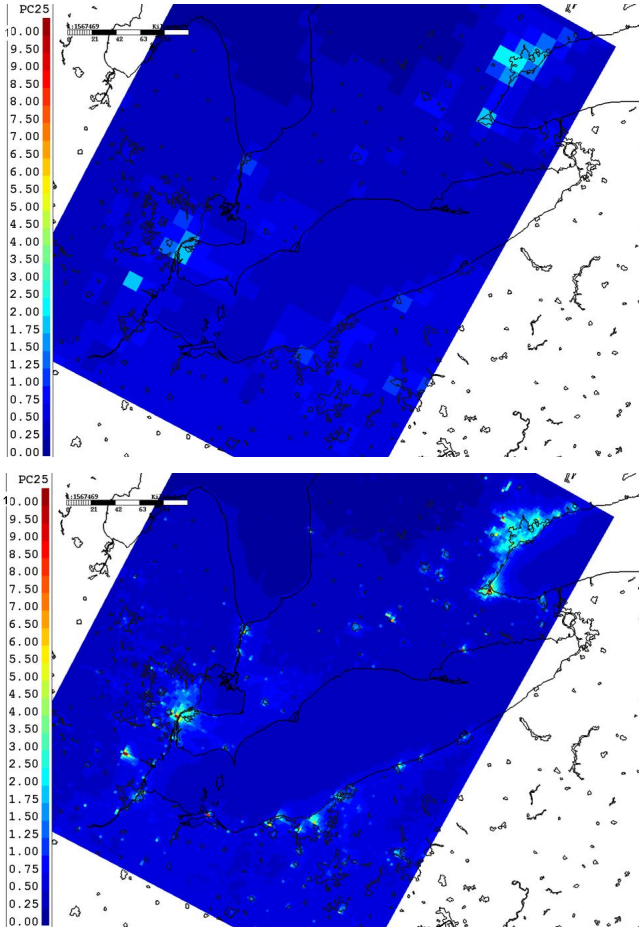

Fig. 6. Same as Fig. 5 but for $PM_{2.5}$ POA results.

ACPD
10, 30347–30379, 2010

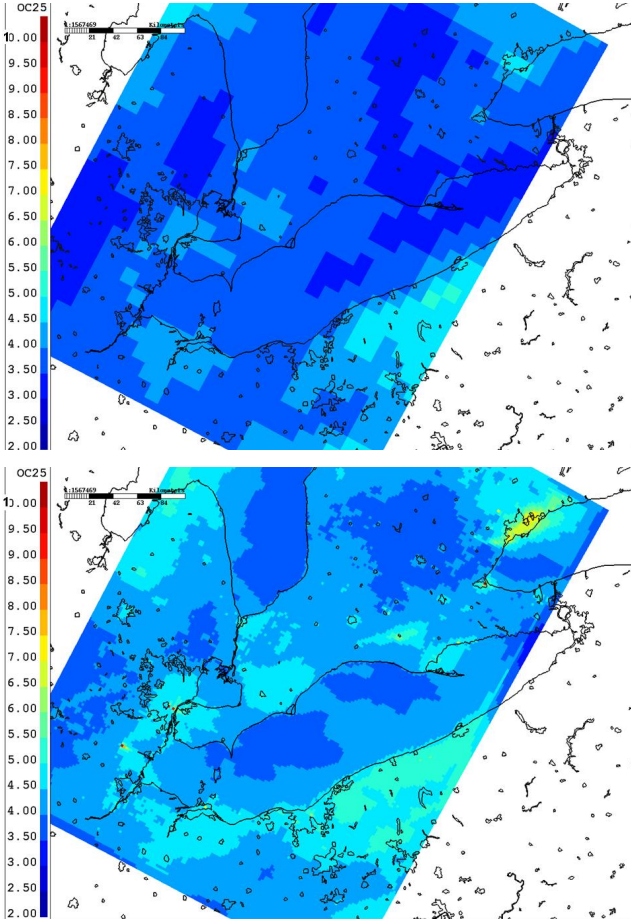

Fig. 7. Same as Fig. 5 but for $PM_{2.5}$ SOA results.

ACPD
10, 30347–30379, 2010

Impact of model grid spacing on regional- and urban-scale air quality predictions

C. A. Stroud et al.